X-ray Spectra and Pulse Frequency Changes in SAX J2103.5+4545

A. Baykal

Middle East Technical University, Physics Department, 06531 Ankara, Turkey

altan@astroa.physics.metu.edu.tr

M. J. Stark

Department of Physics, Lafayette College, Easton, PA 18042, USA

starkm@lafayette.edu

and

J. H. Swank

Laboratory for High Energy Astrophysics, NASA Goddard Space Flight Center, Greenbelt, MD 20771, USA

swank@milkyway.gsfc.nasa.gov

ABSTRACT

The November 1999 outburst of the transient pulsar SAX J2103.5+4545 was monitored with the large area detectors of the Rossi X-Ray Timing Explorer until the pulsar faded after a year. The 358 s pulsar was spun up for 150 days, at which point the flux dropped quickly by a factor of ≈ 7, the frequency saturated and, as the flux continued to decline, a weak spin-down began. The pulses remained strong during the decay and the spin-up/flux correlation can be fit to the Ghosh & Lamb derivations for the spin-up caused by accretion from a thin, pressure-dominated disk, for a distance ≈ 3.2 kpc and a surface magnetic field $\approx 1.2 \times 10^{13}$ Gauss. During the bright spin-up part of the outburst, the flux was subject to strong orbital modulation, peaking ≈ 3 days after periastron of the eccentric 12.68 day orbit, while during the faint part, there was little orbital modulation. The X-ray spectra were typical of accreting pulsars, describable by a cut-off power-law, with an emission line near the 6.4 keV of K_α fluorescence from cool iron. The equivalent width of this emission did not share the orbital modulation, but nearly doubled during the faint phase, despite little change in the column

density. The outburst could have been caused by an episode of increased wind from a Be star, such that a small accretion disk is formed during each periastron passage. A change in the wind and disk structure apparently occurred after 5 months such that the accretion rate was no longer modulated or the diffusion time was longer. The distance estimate implies the X-ray luminosity observed was between 1×10^{36} ergs s^{-1} and 6×10^{34} ergs s^{-1}, with a small but definite correlation of the intrinsic power-law spectral index.

Subject headings: X-ray binaries: stars: individual (SAX J2103.5+4545) – stars: neutron – X-rays: stars

1. Introduction

The transient X-ray source SAX J2103.5+4545 was discovered by the Wide Field Camera instrument on the BeppoSAX X-ray satellite during the outburst between February and September 1997 (Hulleman, in 't Zand, & Heise 1998). The source showed 358.61 s pulsations. The X-ray spectrum was consistent with a power-law model. The photon index was 1.27 ± 0.14 and the absorption column density was $3.1 \pm 1.4 \times 10^{22}$ cm^{-2}.

Another outburst was detected 2 years later by the All-Sky Monitor (ASM) on the Rossi X-Ray Timing Explorer (RXTE). Pointed observations were carried out with RXTE. Doppler shifts of the pulsations seen in these observations revealed that the orbital period is 12.68 days (Baykal, Stark & Swank 2000a,b). The orbital parameters suggest that the source has a high mass companion, but no suitable optical counterpart has been reported. Hulleman et al. (1998) pointed out a B star at the edge of BeppoSAX error box, but its distance would imply a luminosity too low to explain the spin-up that was seen in the initial RXTE observations.

SAX J2103.5+4545 continued to be active more than a year after the ASM detectors detected it in 1999 November. During the active interval the source was monitored through regular pointed RXTE observations. In this work, we present results from analysis of the X-ray spectra as well as new results from the pulse timing of the full set of observations. During this outburst, although the source is not a bright target ($\leq$ 30 mCrab), it was possible to make very significant measurements which have a bearing on several aspects of accreting pulsars.

2. Observations and data analysis

SAX J2103.5+4545 was regularly observed between 19/11/99 and 31/08/00. Approximately 3-4 daily observations took place per week with a total weekly exposure time of 10-15 ks. Between 12/09/00 and 02/12/00, the observations were separated by a few weeks. In March 2001, the source began another outburst. RXTE carried out a few observations 30 days after. The total nominal exposure time of the observations was 521 ks. The results presented here are based on data collected with the Proportional Counter Arrary (PCA) (Jahoda et al. 1996) and the High Energy X-ray Timing Experiment (HEXTE) (Rothschild et al. 1998). The PCA instrument consists of an array of five collimated xenon/methane multi-anode proportional counters, although they were not all operated during some observations. The total effective area is approximately 6250 cm^2 and the field of view $\sim 1^\circ$ full width at half maximum (FWHM). The HEXTE instrument consists of two independent clusters of detectors, each cluster containing four NaI(T1)/CsI(Na) phoswich scintillation counters (one of the detectors in cluster 2 not used for spectral information) sharing a common $\sim 1^\circ$ FWHM field of view. The field of view of each cluster is switched on and off source to provide background measurements. The net open area of the seven detectors used for spectroscopy is 1400 cm^2. Each detector covers the energy range 15-250 keV.

2.1. X-ray light curves and spectra

Background light curves and X-ray spectra were generated by using the background estimator models based on the rate of very large events (VLE), detector activation and cosmic X-ray emission. The background light curves were subtracted from the source light curve obtained from the binned GoodXenon data. Figure 1 presents the light curve per proportional counter unit (PCU). From this figure, it is clear that the count rate dropped after the first 150 days of observations. Background subtracted spectra for each active PCU were combined with FTOOLS software provided by the RXTE Guest Observer Facility of HEASARC. For the HEXTE data the background subtraction is straightforward since the HEXTE detectors are rocking on and off the source at 32 s intervals. Standard FTOOLS software was used for the HEXTE data reduction, including the deadtime correction. We modelled the X-ray spectra of the PCA and HEXTE together between 3 and 50 keV, using a power-law function with low-energy absorption (Morrison & McCammon 1983), multiplied with an exponential high-energy cut-off function (White, Swank, & Holt 1983). The fits required an emission line consistent with the 6.4 keV of fluorescence from cold iron. We checked that at the galactic longitude (87.13°) and latitude (−0.68°) of SAX J2103.5+4545 the contribution of galactic ridge emission is small. Pointed observations nearby and scans

in the region imply no more than 0.2 counts s^{-1} per PCU, less than half of the minimum rate detected at the end of the outburst, when the pulse period was still measured, and too small to influence the spectrum extracted for the faint phase. We studied the X-ray spectra in the bright phase of the outburst (< 150 days) and in the faint phase of the outburst (> 150 days) independently. Table 1 presents the best fit values. The photon index and the line parameters changed significantly. The photon index (Γ=1.27 $\pm$ 0.02) in the bright phase was consistent with the index found by BeppoSAX in the preceeding outburst. It was lower (flatter spectrum) than the index in the faint phase (Γ=1.41 $\pm$ 0.04). The emission line energy did not change significantly, but the line flux halved, while the equivalent width increased. Figure 2 shows the joint X-ray spectra of RXTE/PCA and HEXTE during the bright phase. Thermal bremsstrahlung models did not give successful fits to the data.

In order to see the other variations in the spectral parameters on shorter time scales, we present in figure 3 the count rates and the best fit spectral parameters in the 3–20 keV range as a function of time, with the time resolution of approximately one week. We do not see significant changes in spectral parameters, with an exception of a decrease in power-law index at the brightest part of the observations, 100–150 days after the onset.

2.2. Orbital Phase Spectra

In our earlier study of this source, we saw an increase in the count rate at periastron passages (Baykal, Stark, & Swank 2000b). This behaviour implied that the mass accretion rate onto the neutron star increases at periastron passage due to the eccentric orbit (e=0.4 $\pm$0.2). We now find that when we fold the faint parts of the outburst on the orbital period of 12.68 days, we do not see any change in the count rate as a function of orbital phase. We confirmed this behavior by extracting the ASM data and folding at the orbital period. When we fold either the ASM or the PCA data in the bright phase, we see a significant orbital modulation, while for the faint phase we do not. Figure 4 presents the best fit spectral parameters as a function of orbital phase in the bright phase of outburst. In this figure, an orbital phase of 0.4 $\pm$ 0.08 corresponds to the periastron passage of the neutron star, and clearly the X-ray flux is higher there, although it actually peaks 2-3 days later. The other spectral parameters do not show significant changes, with the exception of the power-law index. Figure 5 presents the power-law index, the equivalent width and the emission line flux as a function of X-ray flux. In this figure, the power-law index decreases with increasing X-ray flux. In other words the X-ray spectrum becomes harder when the X-ray flux is high and softer when the X-ray flux is low. The emission line flux is proportional to the overall X-ray flux, with the equivalent width consistent with being constant.

2.3. Pulse Frequencies and Pulse Frequency Derivatives

For the timing analysis, we corrected the light curves to the barycenter of the Solar system and then corrected for the binary motion of the pulsar using the binary orbital parameters deduced by Baykal, Stark, & Swank (2000b). We divided the total observation time span into non-overlapping segments of 15–20 days. For each observation segment, we first obtained the nominal pulse frequency (or pulse period) by using a long Fourier transform (or power spectrum) and then constructed 10-20 pulse profiles (one pulse profile for each RXTE orbit) by folding the data at this nominal pulse period. Finally we found the pulse phase offsets (or pulse arrival times) by cross correlating the pulse profiles with a template chosen as the most statistically significant pulse profile in each observation segment. We used the harmonic representation of pulse profiles (Deeter & Boynton 1985). In this technique, the pulse profiles are expressed in terms of a harmonic series and cross correlated with the template pulse profile. The pulse phase offsets can be found in terms of a Taylor expansion,

$$\delta\phi = \phi_0 + \delta\nu(t - t_0) + \frac{1}{2}\dot{\nu}(t - t_0)^2 \qquad (1)$$

where $\delta\phi$ is the pulse phase offset deduced from the pulse timing analysis, t_0 is the mid-time of the observations, ϕ_0 is the phase offset at t_0, $\delta\nu$ is the deviation from the mean pulse frequency (or additive correction to the pulse frequency), and $\dot{\nu}$ is the source's pulse frequency derivative. We fitted the phase offsets to the Taylor expansion given in equation 1. Figure 6 (middle panel) shows the resulting 15 pulse frequency derivatives as a function of the mid-times of the observations. We made linear fits to the phase offsets (i.e. $\delta\phi = \phi_0 + \delta\nu(t - t_0)$) with nearly weekly time resolution, obtaining 31 pulse frequencies. These are shown in the upper panel in figure 6. The lower panel in figure 6 shows the X-ray fluxes associated with the pulse frequency derivatives. Figure 7 shows that the pulse frequency derivatives are clearly correlated with their associated X-ray flux values.

3. Discussion

A correlation between spin-up rate and X-ray flux in different energy ranges has been observed in outbursts of 5 transient systems. These systems are EXO 2030+375, (Parmar, White & Stella 1989, Parmar et al. 1989, Reynolds et al. 1996), 2S 1417-62 (Finger, Wilson & Chakrabarty 1996), A 0535+26 (Bildsten et al. 1997, Finger, Wilson & Harmon 1996), GRO J1744-28 (Bildsten et al. 1997) and XTE J1543-568 (In 't Zand, Corbet & Marshall 2001). All these sources were observed during spin-up phases and the correlations between spin-up rate and X-ray luminosity were explained in terms of accretion from an accretion disk. The outburst of SAX J2103.5+4545 started with a spin-up trend, made a transition

to a steady spin rate and then appeared to just begin a spin-down trend (see figure 7). These measurements of SAX J2103.5+4545 are the first which have resolved the transition to spin-down.

If the accretion is from a Keplerian disk, at the inner disk edge the magnetosphere disrupts the Keplerian rotation of the disk, forcing matter to accrete along magnetic field lines. The inner disk edge r_0 moves inward with increasing mass accretion rate. The dependence of the inner disk edge r_0 on the mass accretion rate $\dot{M}$ may be approximately expressed as (Pringle & Rees 1972, Lamb, Pethick, & Pines 1973)

$$r_0 = K\mu^{4/7}(GM)^{-1/7}\dot{M}^{-2/7} \tag{2}$$

where μ=BR^3 is the neutron star magnetic moment with B the magnetic field and R the neutron star radius, G is the gravitational constant, and M is the mass of the neutron star. In this equation $K = 0.91$ gives the Alfven radius for spherical accretion. Then the torque estimate is given by Ghosh & Lamb (1979) as

$$2\pi I\dot{\nu} = n(w_s)\dot{M}\ l_K, \tag{3}$$

where I is the moment of inertia of the neutron star, $l_K = (GMr_0)^{1/2}$ is the specific angular momentum added by a Keplerian disk to the neutron star at the inner disk edge r_0;

$$n(w_s) \approx 1.4(1 - w_s/w_c)/(1 - w_s) \tag{4}$$

is a dimensionless function that measures the variation of the accretion torque as estimated by the fastness parameter

$$w_s = \nu/\nu_K(r_0) = (r_0/r_{co})^{3/2} = 2\pi K^{3/2}P^{-1}(GM)^{-5/7}\mu^{6/7}\dot{M}^{-3/7}, \tag{5}$$

where $r_{co} = (GM/(2\pi\nu)^2)^{1/3}$ is the corotation radius at which the centrifugal forces balances the gravitational forces, w_c is the critical fastness parameter at which the accretion torque is expected to vanish. The critical fastness parameter w_c has been estimated to be ~ 0.35 and depends on the electrodynamics of the disk (Ghosh & Lamb 1979, Wang 1987, Ghosh 1993, Torkelsson 1998).

The behavior of the dimensionless function n as a function of ω_s can be understood as follows. The accretion torque is the sum of the torque produced by accretion of the angular momentum of the matter that falls onto the star (mechanical torque) and the torque contributed by the twisted magnetic field lines from the star that interact with the outer parts of the disk (magnetic torque). The mechanical torque always acts to spin-up a star rotating in the same sense as the disk flow, whereas torque from the magnetic stresses can have either sign, since the azimuthal pitch of the stellar magnetic field lines that interact with Keplerian

flow in the disk changes sign at the corotation radius r_{co}. The torque from the magnetic field lines threading the disk between the inner disk edge r_0 and corotation radius r_{co} is positive, whereas the contribution of torque from the magnetic field lines threading the disk outside the corotation radius r_{co} is negative. Therefore, either spin-up or spin-down torque is possible in this model as a net effect of the balance between the two contributions. Equation 4 gives an analytic expression approximating numerical calculations of the dimensionless torque (Lamb 1988, Ghosh 1993). The torque will cause a spin-up if the neutron star is rotating slowly ($w_s < w_c$) in the same sense as the circulation in the disk. Even if the neutron star is rotating in the same sense as the disk flow, the torque will be in the direction of spin-down if the neutron star is rotating too rapidly ($w_s > w_c$).

The accreted material will produce X-ray luminosity at the neutron star surface at the rate

$$L = GM\dot{M}/R \tag{6}$$

From equations 2,3 and 6, the rate of spin-up is related to the X-ray intensity through

$$\dot{\nu} \propto n(w_s)L^{6/7} = n(w_s)(4\pi d^2 F)^{6/7}, \tag{7}$$

where d is the distance to the source and F is the X-ray flux.

Since the source distance and magnetic field are not known, we fit the Ghosh & Lamb model of the pulse frequency derivative for these two parameters. Because the power index between the spin-up rate and the X-ray luminosity is a result of the theoretical model, as a test of the model we also fit for this index, obtaining 0.75 ± 0.13, which is consistent with the value 6/7 expected in the model. We obtain for the distance to the source 3.2 ± 0.8 kpc and for the magnetic field $(12 \pm 3) \times 10^{12}$ Gauss. As seen in figure 6, the points corresponding to spin-up and spin-down are consistent with falling on the same curve. With the estimated distance of 3.2 ± 0.8 the source could be in a star formation region in the Perseus arm at approximately 4 kpc (Vogt & Moffat 1975, Georgelin & Georgelin 1976. The X-ray flux at the peak of the outburst $\sim 6.4 \times 10^{-10}$ erg s^{-1} cm^{-2} corresponds to an accretion luminosity of $\sim 8.8 \times 10^{35}$ erg s^{-1} and a mass accretion rate $\sim 6.5 \times 10^{15}$ g s^{-1}). The magnetic field estimate $\sim 12 \times 10^{12}$ Gauss corresponds to a cyclotron emission line at ~ 140 keV, which is too high to be detected by HEXTE, because of the low count rate of the source at this energy range.

During the decrease of mass accretion rate $\dot{M}$, the fastness parameter increases as $w_s \sim \dot{M}^{-3/7}$. When the fastness parameter reaches $w_s = (r_0/r_{co})^{3/2} \sim 0.35$, the inner edge of the disk will be still be well inside the corotation radius $r_0 \sim 0.5 r_{co}$. In this case, even if the net torque on the neutron star vanishes, a large pulse fraction change is not expected, since the polar cap region at which the material accretes and radiates will not be changed

significantly. Figure 8, presents the 3-20 keV pulse profiles at the bright and faint phases of the outburst. It is clearly seen that there is no significant changes in the pulse profiles.

Further decrease of the mass accretion rate eventually will expand the magnetospheric radius $r_m \approx r_0$ to the corotation radius $r_m \sim r_{co}$. Then, some of the material will be accelerated to super-Keplerian velocities and can not easily be accreted. It may be expelled from the system. Accretion of material will carry angular momentum and tend to spin up the neutron star, while the expulsion of matter will extract angular momentum from the star. These forces tend to bring the neutron star into rotation at the equilibrium period. It is expected that accretion is eventually centrifugally inhibited. In this propeller regime the neutron star would rapidly spin-down and the X-ray luminosity might be produced by the release of gravitational energy at the magnetosphere (King & Cominsky 1994, Campana et al. 1995). X-ray luminosity from the magnetospheric emission would be reduced by a factor of $10^3 - 10^4$ (Corbet 1996).

We have assumed here that the accretion is still through a disk. Given that the luminosity is very low ($< 10^{36}$ ergs s^{-1}) and the companion probably an early type star, it is not obvious that the accreting material would be able to form a disk, that is, have enough angular momentum to circularize outside the magnetosphere. Wang (1981) showed that this would be the case if the wind velocity is relatively slow (< 500 km s^{-1}) rather than fast (> 1000 km s^{-1}). The companion is likely to be a Be star, although not yet identified, because these have episodes of dense slow winds in the equatorial plane (Waters et al. 1988; Li & van den Heuvel 1996).

However, if the wind is slow enough that the velocity relative to the neutron star is dominated by the orbital velocity, the accretion would be relatively independent of phase or tend to peak at apastron rather than near periastron as observed. Diffusion through a disk might shift the time of peak X-ray luminosity, but if the shift is as long as a week, the diffusion would also reduce the amplitude of modulation. It is a fast wind with a spherical outflow for which the rate of capture would peak at periastron. What is observed appears to be the opposite of a simple picture of an episode of equatorial slow wind decaying to a fast wind. The phasing of the modulation shown by SAX J2103.5+4545 has been seen for other sources, such as V0332+53 (Waters et al. 1989), in one outburst in which it appeared consistent with prompt response to a wind of about 300 km s^{-1}.

The simple picture does not capture the complexity of Be Star winds. The influence of a wind rotational velocity and a range of velocity laws (or density dependence on distance from the star), in addition to the wind velocity, were studied by Waters et al. (1989). For the SAX J2103.5+4545 outburst that we monitored, a wind velocity of 200-300 km s^{-1} and a typical mass loss rate of $10^{-8} M_\odot$ yr^{-1} of a Be star could give the implied peak

X-ray luminosities, the orbital modulation, and the phase dependence. But the additional parameters would be needed and several different regimes seem possible.

The drop in accretion rate which we observed in SAX J2103.5+4545 coincided with change in the rate of angular momentum exchange. Presumably, both are caused by changes in the wind structure. Exactly what these are is not obvious. The smooth behavior of the angular acceleration of the pulsar, as opposed to erratic (random walk) variations like those of Vela X-1 (Bildsten et al. 1997), for example, implies the accretion is still via a disk. The accretion rate has not yet fallen so low that the propellor effect comes into play. The disk accretion should moderate orbital dependence. For there to be a disk and yet strong orbital modulation at the peak of the outburst, the disk must be small. The lack of modulation at the end of the outburst would be consistent with a disk that is more extensive, through which the diffusion is longer.

Li and van den Heuvel (1996) considered the spin period versus binary period in the diagram first constructed by Corbet (1984). The accretion from a slow wind to a neutron star spinning in equilibrium appears responsible for the main correlation of the Be star systems. Accretion from a fast wind is manifested by supergiants with longer pulse periods for a given orbital period and for Be stars in certain phases. The values of spin and orbital period place SAX J2103.5+4545 among these sources, but a supergiant is usually a steady rather than a transient source. SAX J2103.5+4545 can be viewed as not having yet achieved equilibrium. The transient episode decreased the pulse period by ≈ 0.9 s. If this occurs every 1.4 yr, the source would spin up to the equilibrium line (1–2 s for a 13 d orbital period) in < 600 yr. The frequency value obtained in the 2001 outburst was 1.4×10^{-3} mHz *above* the last previous measurement. It is consistent with an average spin-up rate during the first 30 days (unobserved) of the ourburst being an average of 5×10^{-13} Hz s^{-1}, about the same as in the beginning of the 1999 outburst. The spin-down between the last monitored value in 2000 and the beginning of the 2001 outburst would have been only about 10^{-4} mHz at the rate observed. The spin rate apparently ratchets up with each outburst.

The X-ray spectra in principal can carry information about the disk and the wind as well as about the flow onto the neutron star. The 6.4 keV line, which comes from fluorescence from relatively cold Fe, could come from all of these sources. Fluorescent Fe K_α is common to many high-magnetic-field binary pulsars. The equivalent widths in the bright and faint phase spectra of SAX J2103.5+4545 are similar in magnitude to those observed in spectra of Vela X–1 and GX 301–2 (summarized in Nagase 1989), the accretion rate in SAX J2103.5+4545 is 10–100 times lower and there is no varying column density indicating formation of a shell around the source. Yet for Vela X-1, where the neutron star is eclipsed, the behavior of the line as a function of binary phase implied a source close to the

neutron star in addition to the wind. In the case of SAX J2103.5+4545, the lack of orbital dependence of the equivalent width during the bright part of the outburst again suggests the line is produced close to the neutron star where the geometry of cool material can be independent of the orbital position. In the decaying part of the outburst, the equivalent width is nearly twice as large. The moderate column density implies the material is seen in reflection rather than transmission. The cool fluorescing material may subtend a larger solid angle, or a second component is excited for the new type of wind. The data could not significantly limit orbital modulation of the line emission during this part of the outburst.

The spectral index of the intrinsic X-ray spectrum appears to be consistently correlated with the flux, harder for higher flux, both in the variation with orbital phase and the variation during the outburst. The fact that the pulse amplitude and shape did not change suggests that the X-rays continue to be produced in flow to the neutron star and in that case the X-ray flux seems likely to be proportional to the rate of accretion onto the surface. Intrinsic X-ray spectra for low luminosity sources $\dot{M} < 10^{17}$ g s^{-1} have been modeled (Meszaros et al. (1983); Harding et al. (1984)). The continuum spectrum has not appeared to be very sensitive to the mass accretion rate, but the contributions of the cyclotron line emission were not included and could make a difference if Compton scattering of line photons affects the continuum below the line energy. There has appeared to be at least a relation between the cut-offs observed in pulsar spectra and the cyclotron resonance energies (Makashima & Mihara 1992; see however Mihara, Makashima, & Nagase 1998). The high magnetic field obtained from the spin rate dependence puts the cyclotron resonance energy farther above the cut-off energy than is the case for pulsars with identified resonance features and would give SAX J2103.5+4545 the highest field of the accreting pulsars (Orlandini & Dal Fiume 2001). The magnetic field estimate depends on the critical fastness and the balance between the magnetosphere and the accretion flow. Quantitative estimates seem likely to be subject to dependence of the model on assumptions about the nature of the disk, for example. Understanding the X-ray spectra and flux correlations appears to require better models of the spectral formation and also the magnetospheric physics.

RXTE's monitoring of this transient pulsar allowed the spin rate to be tracked while the luminosity declined to 6×10^{34} ergs s^{-1}. The spin-rate responded smoothly to the flux, spinning up, coming to equilibrium and then reversing sign, just as the Ghosh & Lamb characterization of the magnetospheric interaction predicted. While the magnetic field and distance that come out of fitting the data may be estimates subject to model dependence of the spin-up/flux relation, this source demonstrates the possibility of determining system parameters from such observations. The system is also interesting in that it appears to be different from better known ones and provides information about uncharted parts of parameter space of pulsars in binaries. Detailed study of the orbital phase dependence

during the outbursts of this source will provide constraints on the stellar orbit flows from which this neutron star accretes.

REFERENCES

Baykal, A., Stark, M., & Swank, J. 2000, IAU Circ. 7355

Baykal, A., Stark, M., & Swank, J. 2000, ApJ, 544, L129

Bildsten, L., et al. 1997, ApJS, 113, 367

Campana, S., Stella, L., Mereghetti, S., & Colpi, M. 1995, A&A, 297, 385

Corbet, R.H.D. 1984, A&A, 141, 91

Corbet, R.H.D. 1996, ApJ, 457, L31

Deeter, J.E., & Boynton, P.E. 1985, in Proc. Inuyama Workshop on Timing Studies of X-ray Sources, ed. S. Hayakawa & F. Nagase (Nagoya: Nagoya Univ.), 29

Finger, M.H., Wilson, R.B., & Chakrabarty, D. 1996, A&AS, 120, C209

Finger, M.H., Wilson, R.B., & Harmon, B.A. 1996, ApJ, 459, 288

Georgelin, Y.M., & Georgelin, Y.P. 1976, A&A, 49, 57

Ghosh, P., & Lamb, F.K. 1979, ApJ, 234, 296

Ghosh, P. 1993, The Evolution of X-ray Binaries, College Park, MD, ed. S. S. Holt, & C. S. Day, 439

Harding, A.K., Meszaros, P., Kirk, J.G., & Galloway, D.J. 1984, ApJ, 278, 369

Hulleman, F., in 't Zand, J. J. M., & Heise, J. 1998, A&A, 337, L37

in 't Zand, J.J.M., Corbet, R.H.D., & Marshall, F.E. 2001, ApJ, in press

Jahoda, K., Swank, J., Giles, A.B., Stark, M., Strohmayer, T., & Zhang, W. 1996, Proc, SPIE, 2808,59

King, A., & Cominsky, L. 1994, ApJ, 435, 411

Lamb, F.K. 1988, Timing Neutron Stars, edited by, H.Ögelman & E.P.J. van den Heuvel, NATO ASI Series, vol. 262, pg 649

Lamb, F.K., Pethick, C.J., & Pines, D. 1973, ApJ, 184, 271

Li, X.D., & van den Heuvel E.P.J. 1996, A&A, 314, L13

Meszaros, P., Harding, A.K., Kirk, J.G., & Galloway, D.J. 1983, ApJ, L33, 266

Makashima, K., & Mihara, T. 1992, in Frontiers of X-Ray Astronomy, ed. Y. Tanaka & K. Koyama, Universal Academic Press Inc., Tokyo, 23

Mihara, T., Makishima, K., & Nagase, F. 1998, Adv. Space Res., 22, 987

Morrison, R., & McCammon, D. 1983 ApJ, 270, 119

Nagase, F. 1989, PASJ, 41, 1

Orlandini, M., & Dal Fiume, D. 2001, to be published in Proc. of Bologna Conference; preprint (astro-ph/0107531)

Parmar, A.N., White, N.E., & Stella, L. 1989, ApJ, 338, 373

Parmar, A.N., White, N.E., & Stella, L., Izzo, C., & Ferri, P. 1989, ApJ, 338, 359

Pringle, J.E., & Rees, M.J. 1972, A&A, 21, 1

Reynolds, A.P., Parmar, A.N., Stollberg, M.T., Verbunt, F., Roche, P., Wilson, R.B., & Finger, M.H. 1996, A&A, 312, 872

Rothschild, R.E. et al., 1998 ApJ, 496, 538

Torkelsson, U. 1998, MNRAS, 298, L55

Vogt, N., & Moffat, A.F.J. 1975, A&A, 39, 477

Wang, Y.M. 1981, A&A, 102, 36

Wang, Y.M. 1987, A&A, 183, 257

Waters, L.B.F.M., de Martino, D., Habets, G.M.H.J., & Taylor, A.R. 1989, A&A, 203, 207

Waters, L.B.F.M.,Taylor, A.R., van den Heuvel, E.P.J., Habets, G.M.H.J., & Persi, P. 1988, A&A, 198, 200

White, N.E., Swank, J.H., & Holt, S.S. 1983 ApJ, 270, 711

Fig. 1.— Count rate per PCU history of SAX J2103.5+4545 in 3-20 keV

Fig. 2.— The RXTE/PCA-HEXTE spectra of SAX J2103.5+4545. The lower panel shows the residuals of the fit in terms of χ^2 values.

Fig. 3.— Top panel: Count rate per PCU history of SAX J2103.5+4545 in 3-20 keV. The errors (not indicated) are typically 1%. Second through seventh panel: time history of hydrogen column density, centroid energy of the emission line, equivalent width of the emission line, power-law photon index, cut off energy and e-folding of cut off energy. For some spectra the emission line or cut off energy measurements are not significant due to small numbers of counts and these data points are not included in these panels. Bottom panel: reduced χ^2 statistic of the relevant spectral fits.

Fig. 4.— Top panel: X-ray flux of SAX J2103.5+4545 in 3-20 keV as a function of orbital phase. Second through seventh panel: hydrogen column density, centroid energy of the emission line, equivalent width of the emission line, power-law photon index, cut off energy and e-folding of cut off energy as a function of orbital phase. Bottom panel: reduced χ^2 statistic of the relevant spectral fits.

Fig. 5.— First through third panel: Power-law photon index, equivalent width of the emission line and emission line flux as a function of X-ray flux.

Fig. 6.— First through third panel: Pulse frequency, pulse frequency derivative and X-ray flux history of SAX J2103.5+4545 as a function of time. The increase at the end is 30 days after the start of the next outburst.

Fig. 7.— Pulse frequency derivative versus X-ray flux of SAX J2103.5+4545, solid line presents the best fitted model to the data.

Fig. 8.— Normalized pulse profiles for the bright (dashed one) and faint phases (solid one) of the outburst in 3-20 keV.

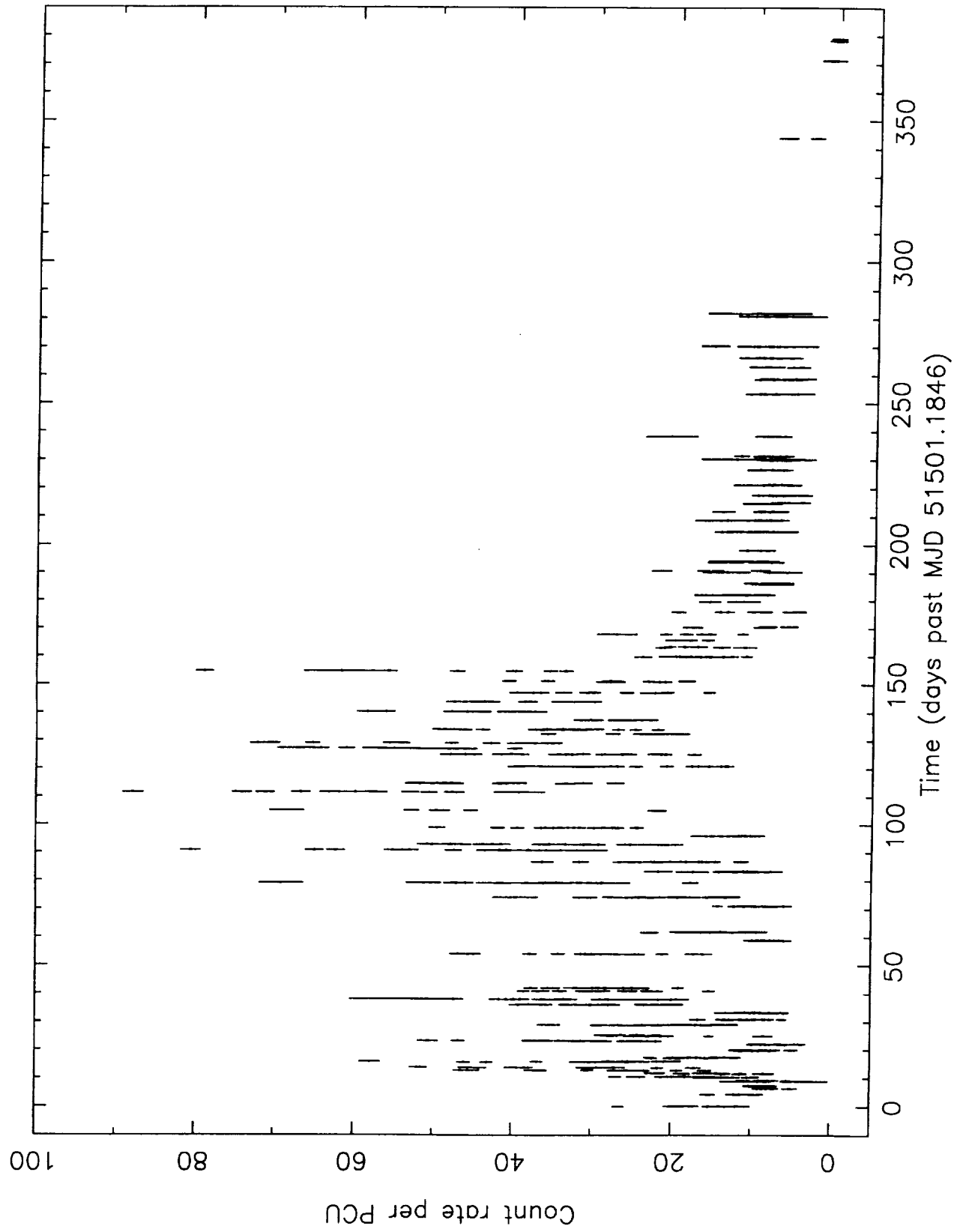
Count rate per PCU
0
20
40
60
80
100
Time (days past MJD 51501.1846)
0
50
100
150
200
250
300
350

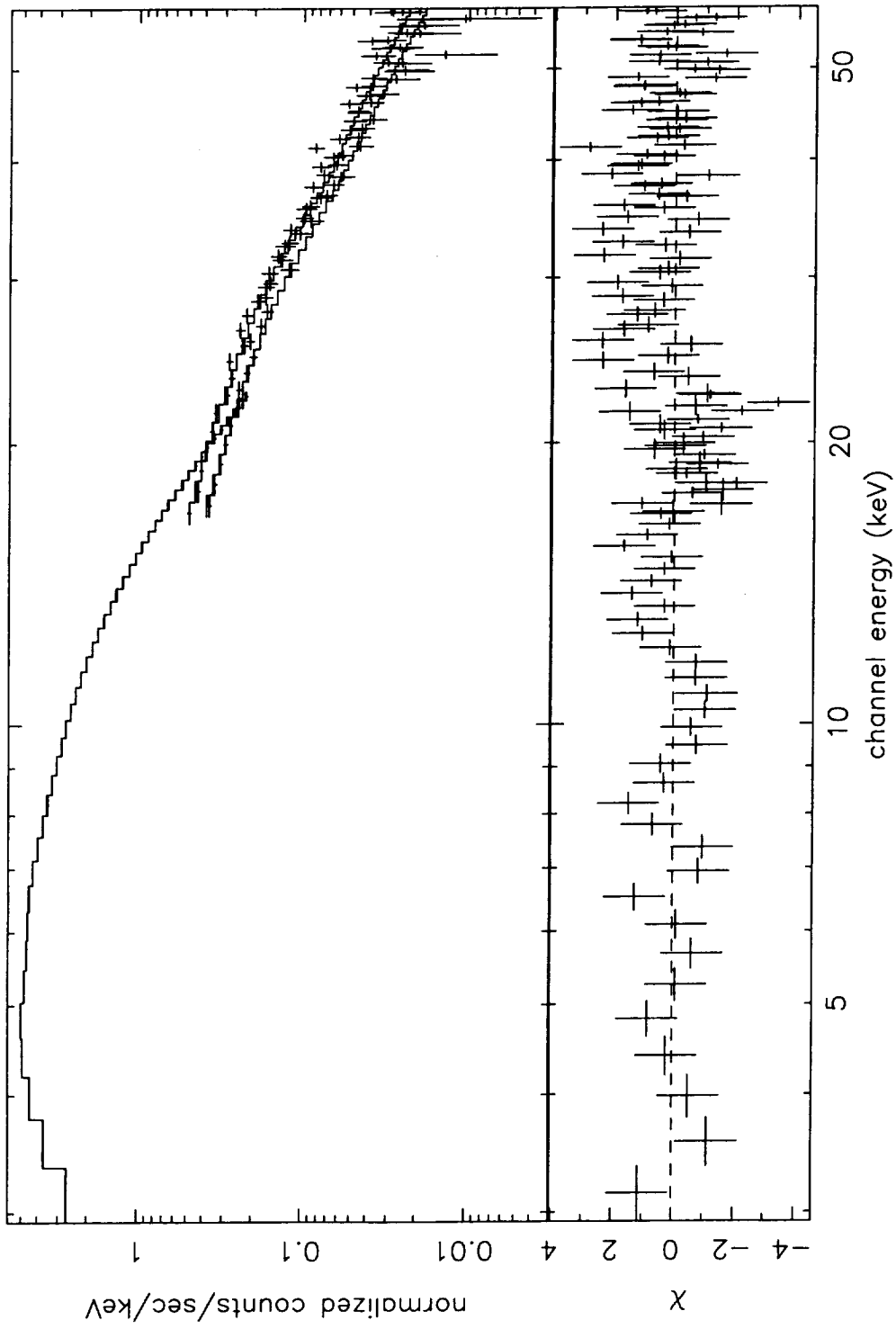
normalized counts/sec/keV
1
0.1
0.01
χ
4
2
0
−2
−4
5
10
20
50
channel energy (keV)

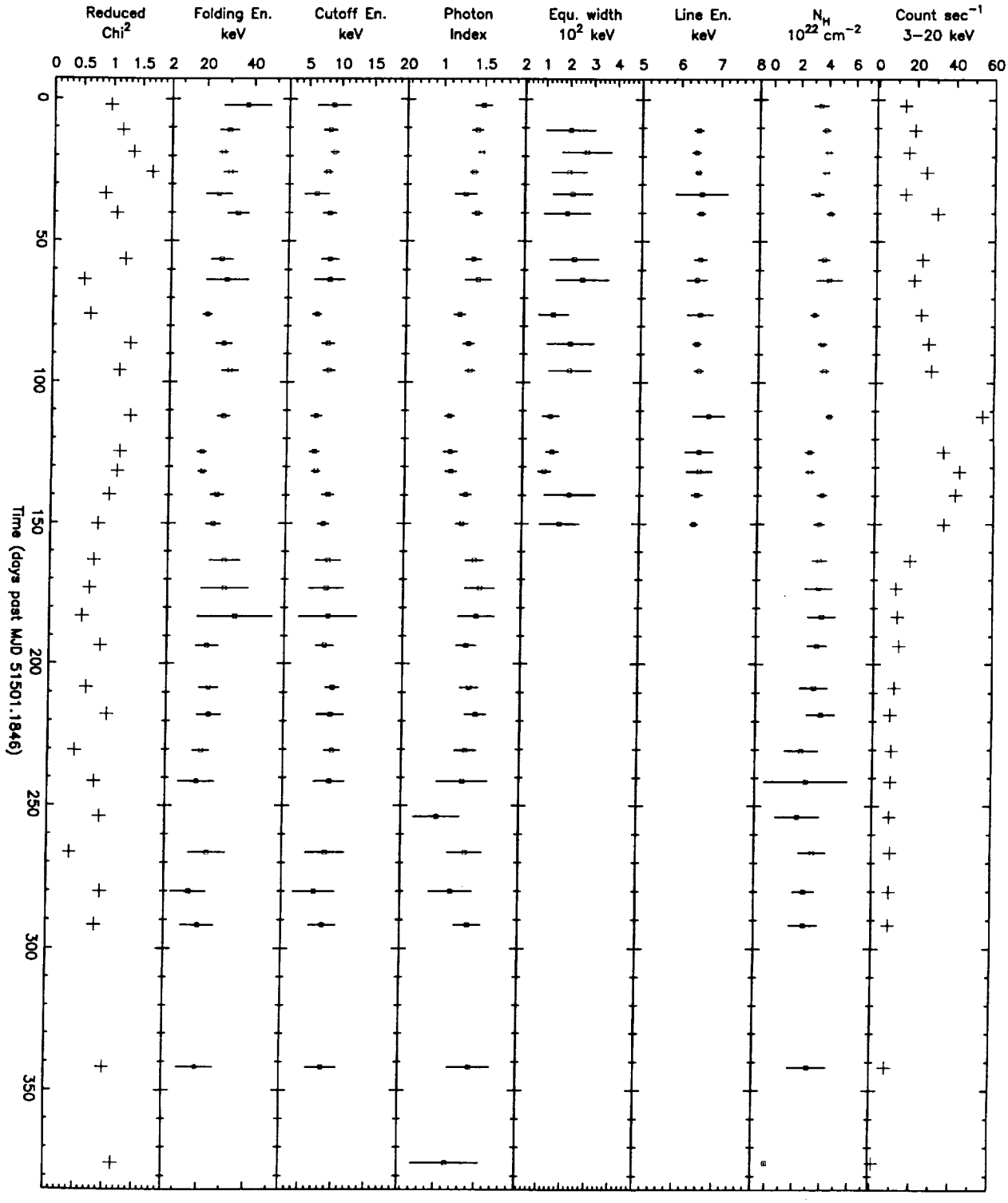
Reduced Chi^2
Folding En. keV
Cutoff En. keV
Photon Index
Equ. width 10^2 keV
Line En. keV
N_H 10^{22} cm^{-2}
Count sec^{-1} 3–20 keV
0 0.5 1 1.5
2 20 40
5 10 15 20
1 1.5 2
2 1 2 3 4 5
6 7 8
0 2 4 6
0 20 40 60
0 50 100 150 200 250 300 350
Time (days past MJD 51501.1846)

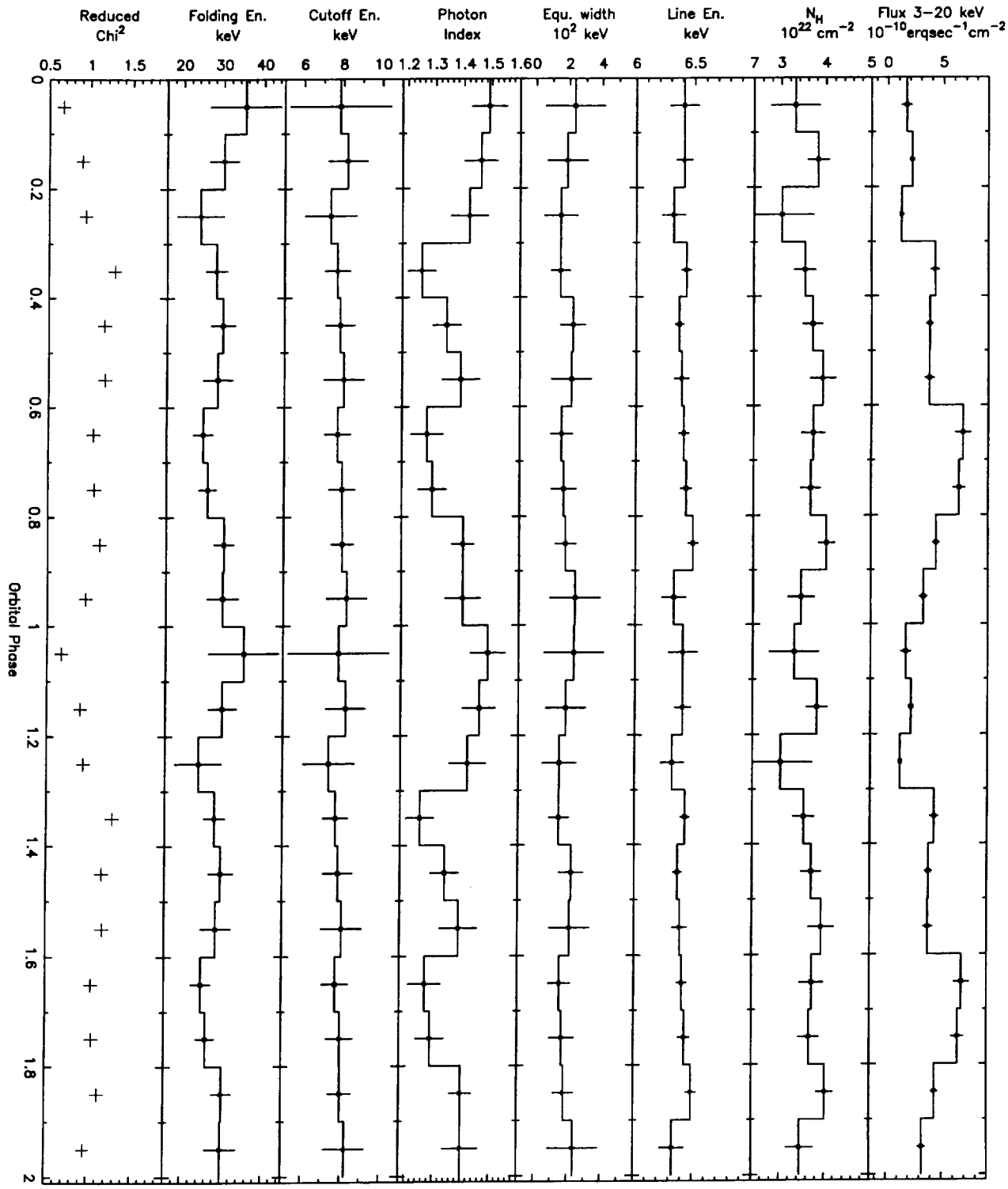
Reduced Chi^2
Folding En. keV
Cutoff En. keV
Photon Index
Equ. width 10^2 keV
Line En. keV
N_H 10^{22} cm^{-2}
Flux 3–20 keV 10^{-10}erqsec^{-1}cm^{-2}
0.5 1 1.5
20 30 40
6 8 10
1.2 1.3 1.4 1.5 1.6
0 2 4 6
6.5
7 3 4
5 0 5
Orbital Phase
0 0.2 0.4 0.6 0.8 1 1.2 1.4 1.6 1.8 2

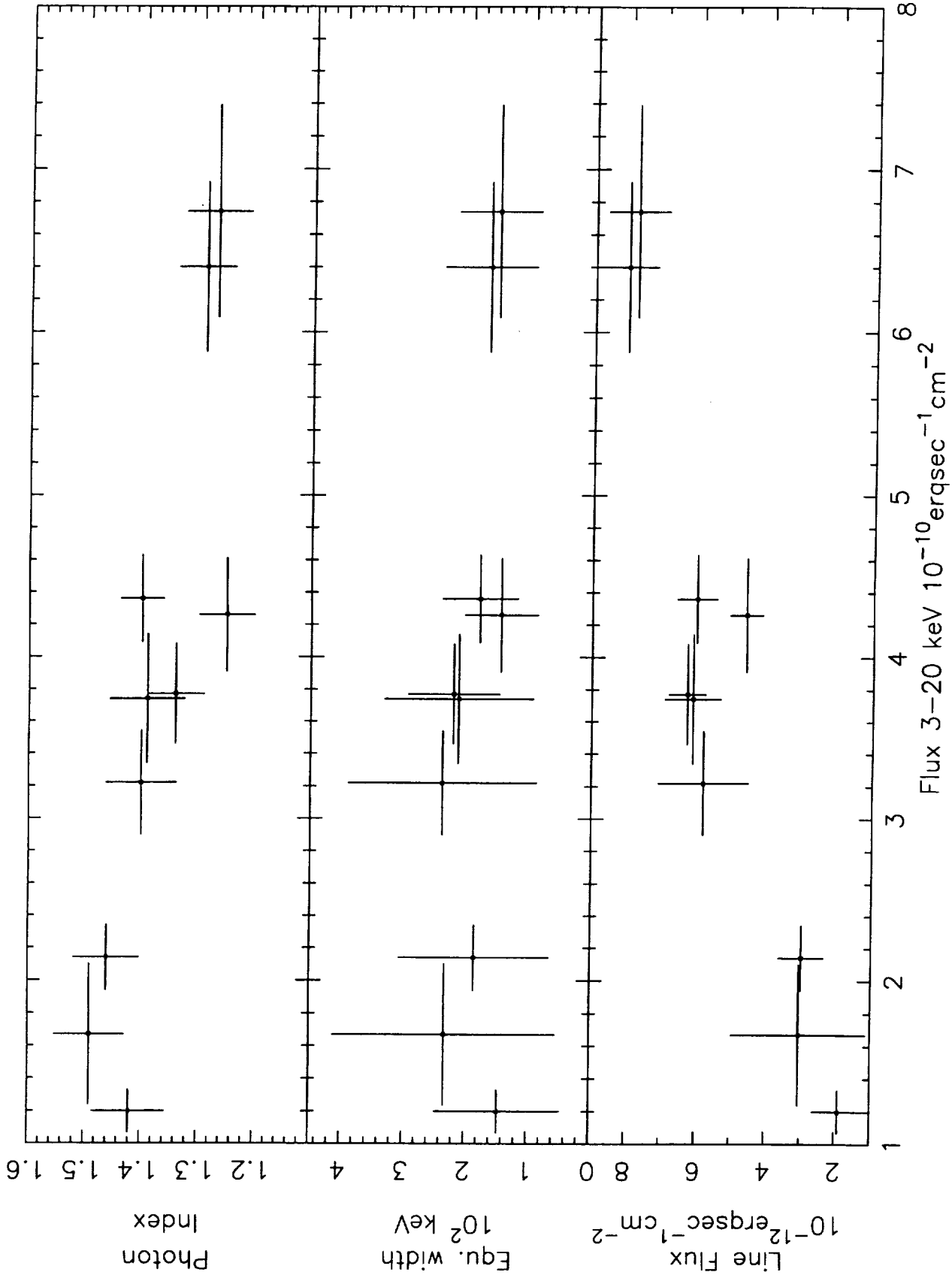
Line Flux
10^{-12}ergsec^{-1}cm^{-2}
Equ. width
10^2 keV
Photon
Index
Flux 3–20 keV 10^{-10}erqsec^{-1}cm^{-2}

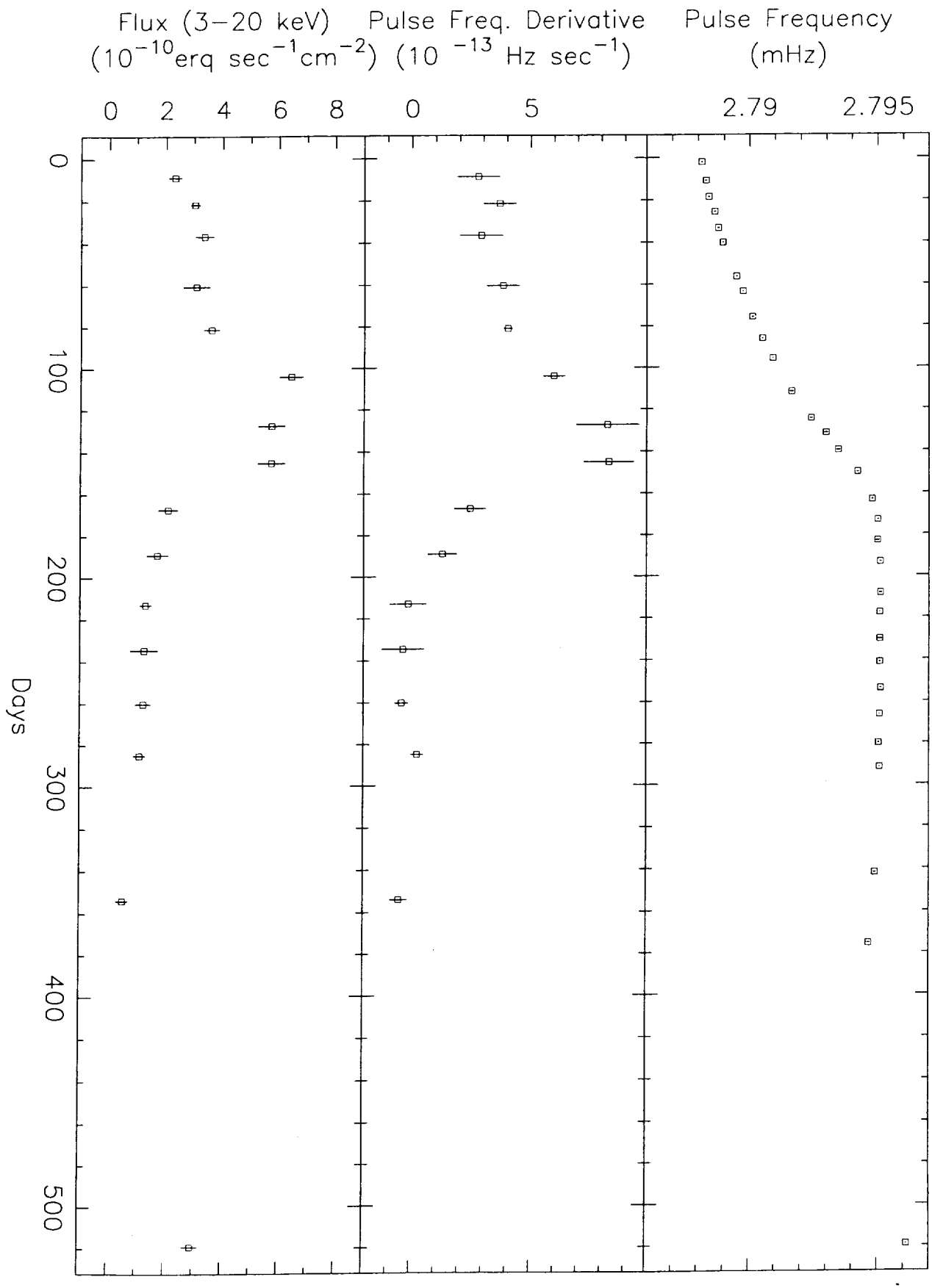
Flux (3–20 keV)
(10^-10 erq sec^-1 cm^-2)
Pulse Freq. Derivative
(10^-13 Hz sec^-1)
Pulse Frequency
(mHz)
0 2 4 6 8
0 5
2.79 2.795
Days
0 100 200 300 400 500

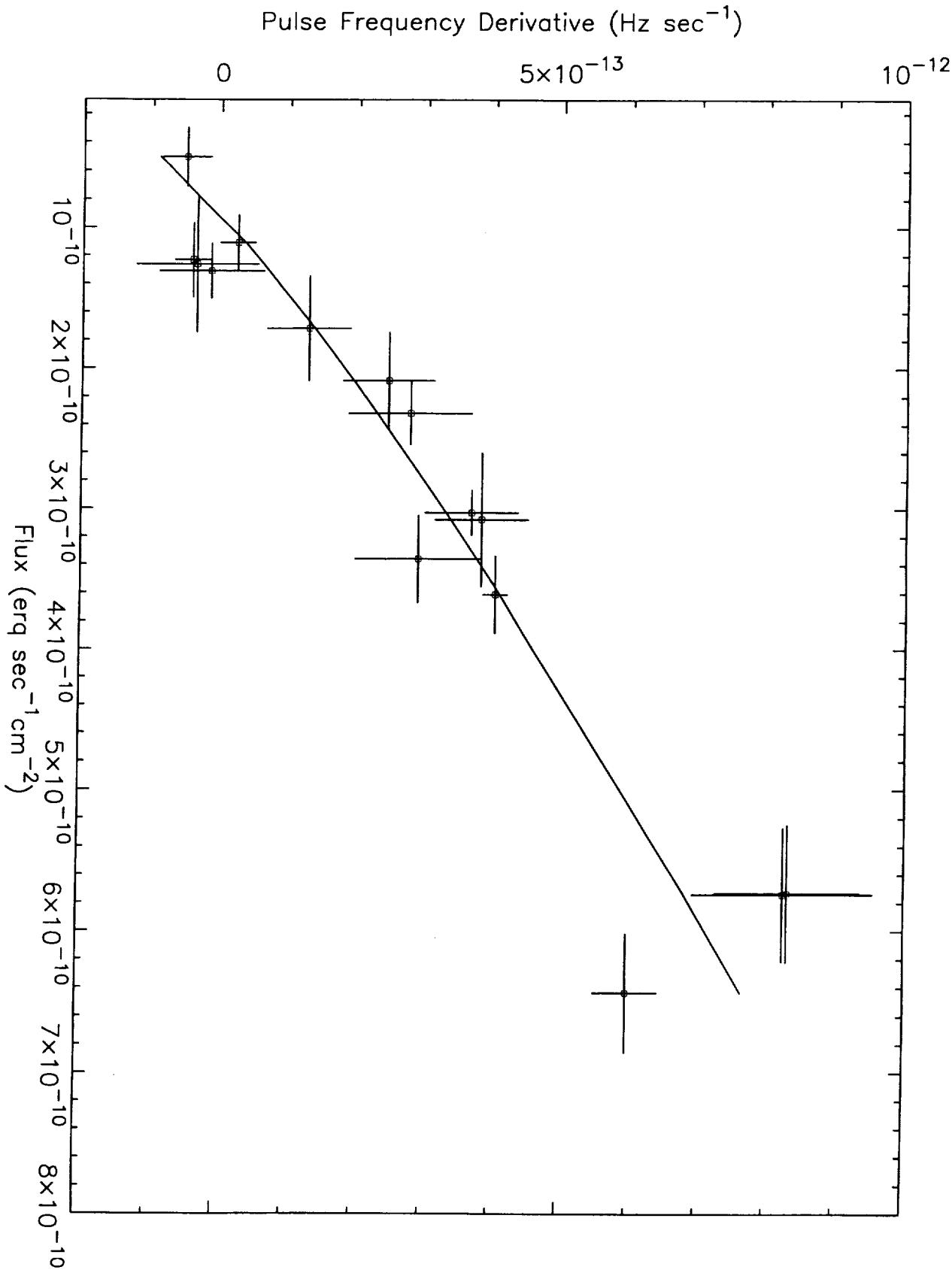
Pulse Frequency Derivative (Hz sec^{-1})
0
5×10^{-13}
10^{-12}
Flux (erg sec^{-1} cm^{-2})
10^{-10}
2×10^{-10}
3×10^{-10}
4×10^{-10}
5×10^{-10}
6×10^{-10}
7×10^{-10}
8×10^{-10}

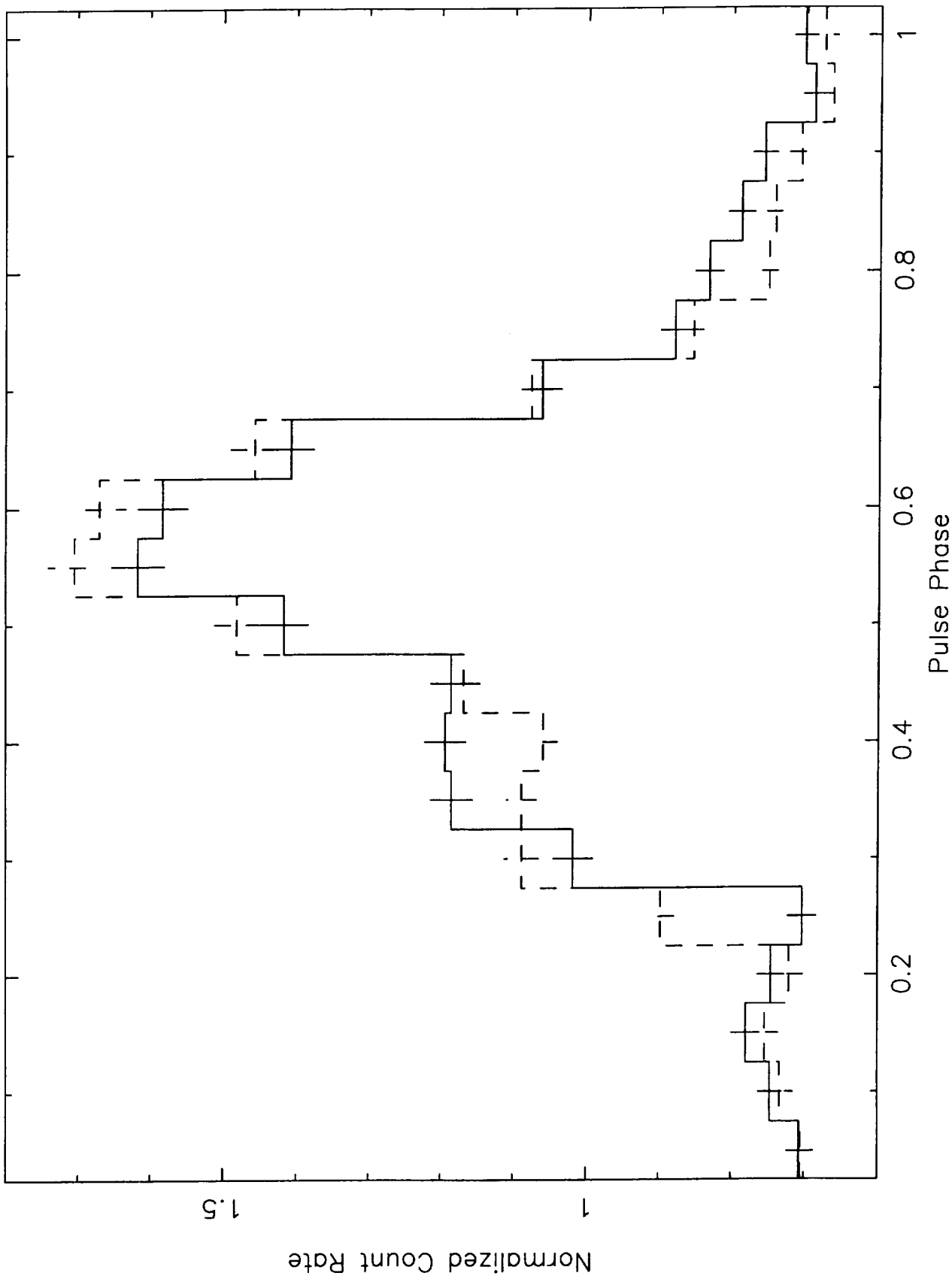
Normalized Count Rate
1.5
1
0.2
0.4
0.6
0.8
1
Pulse Phase

Table 1: Spectral Fit Parameters for RXTE observations[a]

	Bright state	Faint state
N_H (10^{22}cm^{-2})	3.80 ± 0.10	3.65 ± 0.17
Fe line center energy (keV)	6.43 ± 0.02	6.44 ± 0.06
Fe line width (eV)	165 ± 10	306 ± 57
Fe line intensity photons cm^{-2} sec $^{-1}$	(7.61 ± 1.35)× 10^{-4}	(3.12 ± 0.58)×10^{-4}
Photon Index	1.27 ± 0.02	1.41±0.04
Cutoff Energy (keV)	7.89 ± 0.28	7.89[b]
Folding Energy (keV)	27.10 ± 0.94	27.1[b]
Power-law Norm. cm^{-2} at 1keV	(4.84 ± 0.16)× 10^{-2}	(1.41 ± 0.05) × 10^{-2}
Reduced χ^2	1.17 (d.o.f. = 124)	1.2 (d.o.f = 40)

[a] Uncertainties in the spectral fit parameters denote 68% confidence.

[b] HEXTE data are not used at faint state fit because of low count rates. In the fitting procedure, cutoff energy and folding energy are fixed according to values found in bright state.